Environ. Sci. Technol. **2009,** *43,* 350–355

Corrosion and Fate of Depleted Uranium Penetrators under Progressively Anaerobic Conditions in Estuarine Sediment

STEPHANIE HANDLEY-SIDHU,[†] PAUL J. WORSFOLD,[†] CHRISTOPHER BOOTHMAN,[‡] JONATHAN R. LLOYD,[‡] REBECA ALVAREZ,[‡] FRANCIS R. LIVENS,[‡,§] DAVID J. VAUGHAN,[‡] AND MIRANDA J. KEITH-ROACH*,[†]

Biogeochemistry and Environmental Analytical Chemistry Research Group, School of Earth, Ocean and Environmental Sciences, University of Plymouth, Drake Circus, Plymouth PL4 8AA, U.K., Williamson Research Centre for Molecular Environmental Science, School of Earth, Atmospheric and Environmental Sciences, University of Manchester, Manchester M13 9PL, U.K., and Centre for Radiochemistry Research, School of Chemistry, University of Manchester, Manchester M13 9PL., U.K.

Received August 4, 2008. Revised manuscript received October 28, 2008. Accepted November 6, 2008.

The testing of armor-piercing depleted uranium (DU) "penetrators" has resulted in the deposition of DU in the sediments of the Solway Firth, UK. In this study, DU-amended, microcosm experiments simulating Solway Firth sediments under high (31.5) and medium (16.5) salinity conditions were used to investigate the effect of salinity and biogeochemical conditions on the corrosion and fate of DU, and the impact of the corroding DU on the microbial population. Under suboxic conditions, the average corrosion rates were the same for the 31.5 and 16.5 salinity systems at 0.056 ± 0.006 g cm^{-2} y^{-1}, implying that complete corrosion of a 120 mm penetrator would take approximately 540 years. Under sulfate-reducing conditions, corrosion ceased due to passivation of the surface. Corroding DU resulted in more reducing conditions and decreased microbial diversity as indicated by DNA sequencing and phylogenetic analysis. The lack of colloidal and particulate DU corrosion products, along with measurable dissolved U and a homogeneous association of U with the sediment, suggest that U was transported from the penetrator surface into the surrounding environment through dissolution of U(VI), with subsequent interactions resulting in the formation of secondary uranium species in the sediment.

Introduction

Depleted uranium (DU), an alloy of uranium metal with ~0.75% Ti, has been used as an armor penetrator due to its high density, hardness, and relatively low cost. It has been introduced into the environment during conflicts and weapons testing. The UK Ministry of Defense has estimated that, since weapons testing began at their firing range near Kirkcudbright in Scotland in the early 1980s, approximately 30 tonnes of DU has been fired into adjacent Solway Firth waters (*1*). Another test fire range at the Aberdeen Proving Ground in the U.S. resulted in the deposition of >70 tonnes of DU into ecosystems of varying salinity (*2*).

Uranium metal in aqueous systems can experience corrosion or passivation, depending on conditions (*3*). During corrosion there is degradation of the metal, whereas during passivation the metal can become coated with an oxide, hydroxide, hydride or a salt, giving varying degrees of protection against corrosion (*3*). Laboratory-based dissolution studies (*4, 5*) showed that DU-Ti alloy tends to undergo pitting corrosion in the presence of chloride with corrosion rates increasing with Cl^- concentration. Corrosion rates were 0.07 g cm^{-2} y^{-1} in H_2O, which increased to 0.40 g cm^{-2} y^{-1} in 3.5% NaCl (*4*). Another study showed that the corrosion rate increased further in 5% NaCl to 1.47 g cm^{-2} y^{-1} (*5*). The corrosion and dissolution of DU occurs in two stages; first, oxidation of zerovalent U to U(IV), and then oxidation of U(IV) to U(VI). The first process is favorable under all Earth surface conditions, and the second is dependent on redox and pH conditions (*6*). Once corroded, the mobility of uranium is dependent upon its oxidation state, with U(VI) more soluble than U(IV) (*6*). In environments containing (bi)carbonate, stable, mobile uranyl(U(VI)) complexes such as $UO_2(CO_3)_2^{2-}$ or $UO_2(CO_3)_3^{4-}$ form (*6*).

The long-term fate of unfired DU−Ti alloy in the water column and muddy fine grained Solway Firth surface sediments have been investigated through in situ studies (*7*). In both the water column and sediment experiments, scattered pits developed on the DU surface, with black uraninite (UO_2) corrosion products adhering to the surface. The reported corrosion rates were 2.9 g cm^{-2} y^{-1} in the water column and 1.6 g cm^{-2} y^{-1} in the sediment; however, the redox conditions were not determined. The sediment of the Solway Firth seabed is highly variable, ranging from fine to coarse grains (*7*). The fine grained, organic-rich marine sediments prevent ready diffusion of oxygen; thus, in these, the biogeochemical environment is controlled by anaerobic respiration processes. Microorganisms in the sediments utilize a succession of terminal electron acceptors (TEAs) for the oxidation of organic matter, with the amount of energy gained from each TEA influencing the rate and sequence of TEA utilization. The classical TEA sequence is O_2, NO_3^-, Mn(IV), Fe(III), SO_4^{2-}, and CO_2 (*8*). The corrosion of U (eq 1) in low O_2 environments is favorable (*9*) and the H_2 released can be used as an electron donor by some microorganisms to support NO_3^-- (*10*), Fe(III)- (*11*), and SO_4^{2-}-reduction (*12, 13*). The geochemical indicators NO_3^-, Fe(III) and SO_4^{2-} can also be reduced abiotically by H_2, as shown in eqs 2−4 (*14*).

$$U + 2H_2O \rightarrow UO_2 + 2H_2 = -139.53\ \Delta G(\text{kJ/mol of } e^-) \quad (1)$$

$$\frac{1}{5}NO_3^- + \frac{1}{5}H^+ + \frac{1}{2}H_2 \rightarrow \frac{1}{10}N_2 + \frac{3}{5}H_2O = -86.44\ \Delta G(\text{kJ/mol of } e^-) \quad (2)$$

$$Fe(OH)_{3(am)} + 2H^+ + \frac{1}{2}H_2 \rightarrow Fe^{2+} + 3H_2O = -43.89\ \Delta G(\text{kJ/mol of } e^-) \quad (3)$$

$$\frac{1}{8}SO_4^{2-} + \frac{1}{8}H^+ + \frac{1}{2}H_2 \rightarrow \frac{1}{8}HS^- + \frac{1}{2}H_2O = -0.42\ \Delta G(\text{kJ/mol of } e^-) \quad (4)$$

* Corresponding author phone: +44 1752 584578; e-mail: mkeith-roach@plymouth.ac.uk.
[†] University of Plymouth.
[‡] School of Earth, Atmospheric and Environmental Sciences, University of Manchester.
[§] School of Chemistry, University of Manchester.

10.1021/es8021842 CCC: $40.75 © 2009 American Chemical Society
Published on Web 12/19/2008

At pH 7 and during O_2, NO_3^-, and Mn(IV) reduction, mobile U(VI) species dominate, while during Fe(III), SO_4^{2-}, and CO_2 reduction, the immobile U(IV) species dominate (*8*). Iron- and sulfate-reducing bacteria can also reduce U(VI) to U(IV) directly by enzymatic action (*15*−*18*), thus the microbial population influences the fate of DU.

There is a need to investigate the corrosion of DU-Ti alloy under conditions such as those in the Solway Firth to define the controls and mechanisms involved. Laboratory microcosm experiments have therefore been carried out to investigate the fate of DU penetrator material in undisturbed estuarine sediment. The aims of the study were to determine (1) the corrosion of DU within Solway Firth sediments under progressively anaerobic conditions, (2) the dissolved and particulate products formed during the corrosion processes, and (3) the impact of DU on the natural microbial community, to test the hypothesis that the rate of DU corrosion, and the corrosion products formed, are dependent on the local biogeochemical conditions.

Experimental Section

Sampling and Characterization. Intertidal estuarine sediment (5 kg) was sampled from Bowness-on-Solway, Solway Firth (Lat: 54.951070 °N Long: 3.214709 °W GB; 02.04.06). Care was taken to collect only the oxic surface layer (0.5 cm), which was light in color. The sediment was homogenized, stored at 10 °C, and used within 2 weeks of collection. Subsamples of the sediment were dried to determine the water content, and the size distribution of the <2 mm dried sediment particles was measured by low angle laser light scattering (Malvern Mastersizer Long-bed X with MS17 autosampler, Worcestershire), in triplicate. Sedimentary organic carbon was quantified using a CHNS analyzer (EA 1110, CE Instruments, Wigan) following removal of inorganic carbon by exposure to 12 M HCl vapor for 48 h. Ethylenediamine tetraacetic acid was used to calibrate the instrument and a certified reference sediment, PACS-1 (National Research Council of Canada), was used to validate the procedure. The cation exchange capacity was determined through exchange with sodium ions (*19*) and the bulk mineral composition of the ground sediment prepared in pellets with Hoechst Wax C Micropowder was determined by X-ray fluorescence (XRF) (Axios, Panalytical, Almelo). The aqueous extractable inorganic carbon from sediment was quantified using a total organic carbon analyzer (T5000; Shimadzu Ltd., Milton Keynes), the instrument was calibrated using potassium hydrogen phthalate.

Seawater was sampled from Plymouth Sound (Lat: 50.460211°N Long: 4.063914 °W GB; 02.04.06) and river water from the River Tamar (Lat: 50.522302 °N Long: 4.209116 °W GB; 02.04.06). These waters were stored at 4 °C and used within one week of collection. The pH of the waters was determined (MI-410, Microelectrodes Inc., NH) using a bench meter, salinity was determined using a portable refractometer (DIGIT-100 ATC, Medline Ltd., Oxford), and chloride, nitrate, and sulfate were quantified by ion chromatography (Dionex IonPac AS9-HC column, Dionex DX-500 system; Dionex Co, Camberley).

Microcosm Experiments. Microcosm experiments were designed to investigate DU corrosion over time in progressively anaerobic estuarine environments. DU penetrator material was supplied by Dstl (Porton Down, UK) and cut into triangular "coupons" (triangular face of ca 1.5 × 1.5 × 1.0 cm, height 0.5 cm and mass 5−10 g) by AWE (Aldermaston, UK). The DU coupons were cleaned prior to use to remove any cutting oil or surface contaminants (*7*). This involved ultrasonication in dichloromethane (10 min), air drying and ultrasonication in isopropanol (10 min). The coupons were air-dried, weighed accurately, and stored in polyethylene bags prior to use. All experimental microcosms were prepared on the same day. These consisted of a 50 mL glass serum bottle (Wheaton Scientific, NJ), 20 g of field moist sediment, and 10 mL of either seawater, to mimic conditions in the Solway Firth, or a 1:1 mix of river and seawater, to mimic areas with a freshwater influence and investigate the effect of salinity on DU corrosion. For each salinity, thirty microcosms containing a DU coupon were prepared, together with an equivalent number of controls without a DU coupon. The microcosms were sealed with a butyl rubber stopper (Bellco Glass Inc., NJ) and aluminum seals (Sigma-Aldrich, Dorset). An 18 gauge needle was inserted and attached to a syringe to prevent pressure build-up (none observed). The microcosms were incubated anaerobically in the dark at 10 °C.

At each time point of interest over a period of 500 days, microcosms were opened for analysis and characterization ("sacrificed") in triplicate, along with three controls. To preserve redox conditions within the microcosms, all sacrifices and further manipulations were carried out within an anaerobic chamber (Coy Laboratory Products Inc., MI; 95% N_2, 5% H_2). The microcosms were mechanically swirled for 15 min at 200 rpm to homogenize the sediment and water, placed in the anaerobic chamber and the butyl rubber stoppers removed. The entire contents of the microcosms were then filtered successively through nylon mesh (65 μm) and a disposable syringe filter (0.45 μm, mixed cellulose esters) and collected in acid-washed polypropylene vials. The DU coupons, solution and sediment were then prepared for further analysis as described below. All errors stated are 1 standard deviation of three replicate microcosms.

DU Coupon Analysis. The DU coupons were retrieved and rinsed with high purity water (MQ water, 18.2 MΩ cm^{-1}) to remove sediment. Since corrosion is greater in water than in air (*4*), coupons were air-dried and stored in a desiccator to prevent further corrosion. For a visual record, coupons were photographed under a light microscope fitted with a digital camera. Selected coupons were imaged by scanning electron microscopy and analyzed using energy dispersive spectroscopy (SEM-EDAX; Jeol JSM-6100, Tokyo). The corrosion products were removed within 1 month by washing the coupon three times for 30 min in 12 M formic acid, rinsing with ethanol, and then dipping the coupons in concentrated nitric acid for 30 s and rinsing with MQ water (*20*). Once dried, the coupons were reweighed to give mass loss (%).

Geochemical Methods. The oxygen content (MI-730; O_2.ADPT, Microelectrodes Inc., NH), pH (MI-410; O_2.ADPT, Microelectrodes Inc., NH) and Eh (MI-800, Microelectrodes Inc., NH) of the solution phase were determined using calibrated electrochemical probes and a bench meter within the anaerobic chamber, and using a subsample from each microcosm. The redox indicators, sulfate and nitrate, were quantified by ion chromatography. Acid-extractable Fe(II) was extracted from the sediments with 0.5 M HCl for 60 min (*21*) and determined by spectrophotometry (562 nm) using the ferrozine method (*22*). The water was filtered (0.45 μm) and ultrafiltered (10 kDa; Vivaspin Sartorius Group, Epsom) to obtain "colloidal" + "dissolved" (<0.45 μm) and "dissolved" (<10 kDa) U fractions. The method of separating DU colloids by ultrafiltration has previously been compared with two other techniques (gel electrophoresis and gel filtration) and all were found to be highly consistent (*23*). These fractions were diluted in 2% (v/v) nitric acid and analyzed for total U by ICP-MS (0.3 μg L^{-1} detection limit, Plasmaquad PQ2+ Turbo; Thermo Elemental, Cheshire), using thorium as the internal standard. Subsamples of the sediment from the day 500 microcosms were refluxed with concentrated nitric acid for 8 h. The total U was analyzed by ICP-OES (0.1 mg L^{-1} detection limit, Varian 725-ES Axial, CA).

Geochemical Modeling. The Hydra hydrochemical database with MEDUSA software (by I Puigdomenech, Inorganic Chemistry Royal Institute of Technology, Stockholm, Sweden)

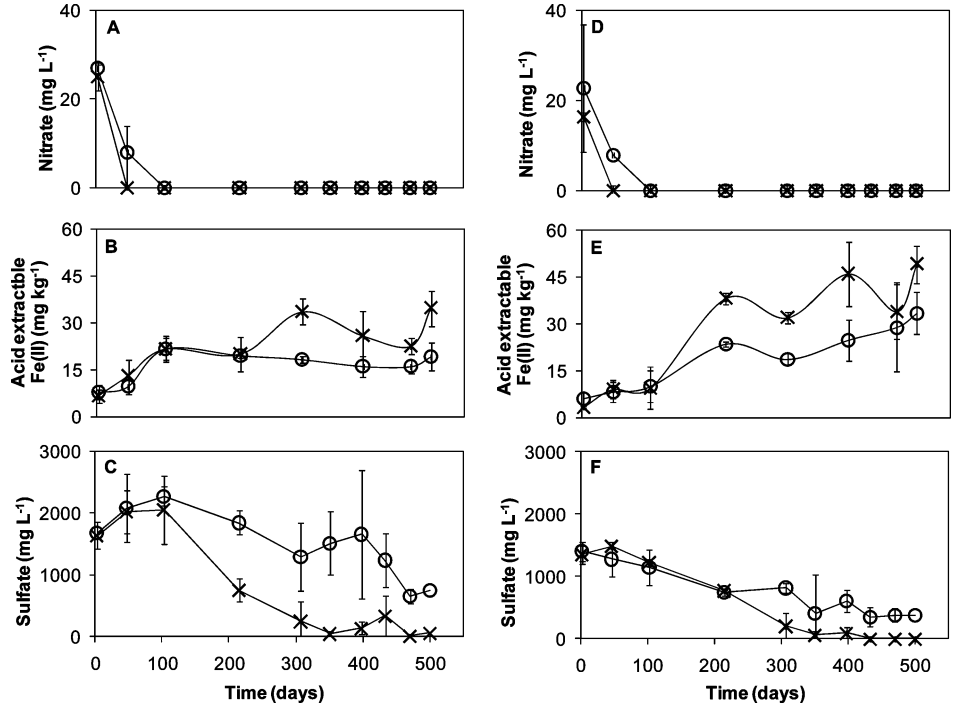

FIGURE 1. Biogeochemical time series data for the high (A−C) and medium (D−F) salinity DU contaminated (×) and control (○) microcosms. (A) and (D) show nitrate concentrations, (B) and (E) acid extractable Fe(II), and (C) and (F) sulfate concentrations over time. Error bars show ± 1 SD ($n = 3$).

was used to model geochemical speciation of U under the experimental Eh and pH conditions.

Microbiological Methods. Three time points of the high salinity series and their controls were selected for ribosomal intergenic spacer analysis (RISA) so that changes in the microbial profile could be identified over time and/or as a result of the presence of DU. DNA was extracted from sediment samples using a Fast DNA spin kit, Powersoil DNA Isolation Kit, (Cambio, Cambridge). The 16S-23S rRNA intergenic spacer region from the bacterial RNA operon was amplified as described previously using primers ITSF and ITSReub (*24*). The amplified products were separated by electrophoresis in Tris-acetate-EDTA gel. DNA was stained with ethidium bromide and viewed under short-wave UV light. Positive microbial community changes identified by the RISA justified further investigation by DNA sequencing of 16S rRNA gene clone libraries and phylogenetic analysis. Here, approximately 1490 base pairs of the 16S rRNA gene was amplified using the broad-specificity 16S rRNA gene primers 8F and 1492R following published PCR reaction conditions (*25*), cloned into a pSC-A-amp/kan cloning vector and reamplified using primers complementary to the flanking regions of the PCR insertion site of the vector. Restriction fragment length polymorphism and DNA sequencing was carried out on the reamplified products (*25*). Sequences (typically 850 base pairs in length) were analyzed against the NCBI (U.S.) database using BLAST program packages and matched to known 16S rRNA gene sequences.

Sediment DU Distribution and Particle Analysis. Approximately 1 g of sediment from day 500 was spread thinly onto a grid plate; a clean phosphor screen was then placed on top for 2 h. The phosphor screen image was recorded on a Typhoon 9410 variable mode imager (Amersham Biosciences, Buckinghamshire). The image was used to identify areas of enhanced radioactivity or "hot" particles, which were subsequently isolated and analyzed by Environmental SEM-EDAX (Philips XL30 ESEM-FEG, OR).

Results and Discussion

Sediment and Water Characterization. The sediment is 31% (m/m) water, with a particle size distribution of 58% sand, 39% silt, and 2.5% clay, organic carbon by mass of 3.2 ± 0.1% and a cation exchange capacity of 4.0 ± 0.4 meq/100 g and an initial inorganic carbon content of 370 ± 20 mg kg^{-1}. Manganese and iron oxides comprised 0.1% (m/m) and 3.3% (m/m) of the sediment, respectively. Due to the low manganese concentrations, Mn(IV) reduction was not considered to be a significant redox process and was not investigated further.

The pH and salinity of the water phases were characterized prior to mixing with the sediment. The high and medium salinity waters were pH 8.0 and 8.1, had salinities of 31.5 and 16.5; and IC content of 72 ± 0.2 and 42 ± 0.1 mg L^{-1}, respectively. The anion concentrations (mg L^{-1}) in the high salinity water were: chloride 21000 ± 14, nitrate 92 ± 0.7; and sulfate 3100 ± 2, and in the medium salinity water were: chloride 10 000 ± 70; nitrate 40 ± 0.8 and sulfate 1600 ± 5.

Redox Indicators. In both the high and medium salinity DU-amended and control experiments, the microcosms became progressively more anaerobic over 500 days as redox indicators were utilized (Figure 1). Accordingly, the Eh values decreased from +400 mV on day 6 to −190 mV on day 500. Dissolved oxygen was fully depleted from the initial value of ~70 to 0% by day 47, and the pH increased over the duration of the experiment from 6.4 to 8.0.

Both the control samples and DU amended microcosms progressed through the redox cascade in order of NO_3^--, Fe(III)-, and then SO_4^{2-}-reduction, indicating microbially active sediments. However, when comparing control and DU-amended microcosms, variations were observed in TEA concentrations over time for both the high and medium salinity series. Nitrate depletion was more rapid in the DU-amended experiments than the controls, and occurred within 47 and 103 days, respectively. Ingrowth of Fe(II) was observed in all sediments by day 47; however, as Fe(III)-reducing conditions progressed, significantly more Fe(II) was observed in the DU-amended sediments. Initially SO_4^{2-} concentrations

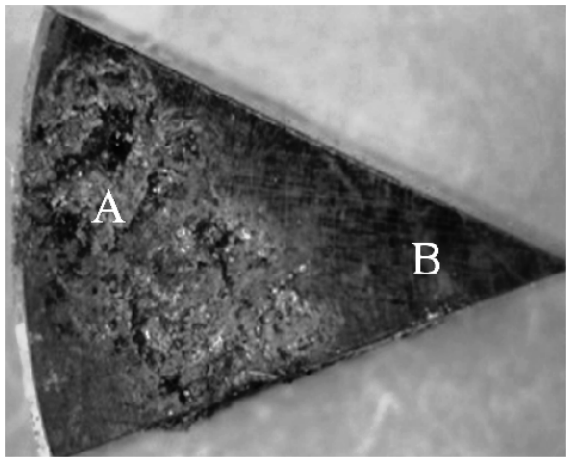

FIGURE 2. Black and white photograph of a DU coupon retrieved from a sulfate-reducing microcosm (day 351), showing (A) areas of heavily pitted corrosion and (B) areas of preserved metal.

increased in the high salinity series, possibly due to desorption or organic sulfur mineralization (*26*). However, SO_4^{2-}-reduction was observed in all sets of microcosms by day 215. Sulfate was then depleted to a greater extent in the DU-amended microcosms than the controls. This increase in NO_3^--, Fe(III)-, and SO_4^{2-}-reduction in the DU-amended experiments can be explained by abiotic or biotic processes. As DU corrodes to UO_2 it releases H_2 which can be used as an electron donor to support microbial NO_3^--reduction (*10*), Fe(III)-reduction (*11*) and SO_4^{2-}-reduction (*12, 13*). The H_2 released can also abiotically reduce NO_3^-, Fe(III), and SO_4^{2-} (see eqs 2−4). Typically in the DU microcosms at day 215, 4.6×10^{-4} moles of U corroded to UO_2, potentially releasing 9.2×10^{-4} moles of H_2 (eq 1). This H_2 is sufficient to reduce 53% of the total NO_3^-, available Fe(III) and SO_4^{2-} abiotically.

Corrosion of DU Coupons. The DU coupons corroded with formation of shallow pits on the surface of the coupon, together with strongly adhering black/gray corrosion products (Figure 2), SEM-EDAX analysis of the coupon surface indicated a uranium oxide, which is most likely to be UO_2; this has previously been reported in a similar DU sediment corrosion study (*7*). Corrosion of DU was observed on day 47 (Figure 3), and then rapid corrosion was observed until day 215. The mass of the coupons did not significantly change in the high ($p = 0.077$) or medium salinity system ($p = 0.47$) from day 215−500. The experimental geochemical conditions (day 215−500; Eh < 0; pH > 7) fall within the zone of uraninite on the relevant Pourbaix diagram (*3*), which suggests that the oxide formation protects against further corrosion by a process of passivation.

The rate of corrosion (g cm^{-2} y^{-1}) was calculated (eq 5). When calculating the surface area of each coupon, the slightly curved side of the coupon was assumed to be straight for simplicity, which introduced a measured uncertainty of ± 2%.

$$\text{corrosion rate (g cm}^{-2}\text{ y}^{-1}) = \frac{365 \times \text{weight loss (g)}}{\text{coupon area (cm}^2) \times \text{time (days)}} \quad (5)$$

$$\text{total corrosion time of 120 mm penetrator} = \frac{4500\text{ (g)}}{\text{corrosion time}} \times \frac{1}{1500\text{ (cm}^2)} \quad (6)$$

The DU coupons corroded measurably when dissolved oxygen concentrations were low and before SO_4^{2-}-reduction was observed, i.e., corrosion occurred predominately under suboxic conditions. The experimental uncertainties on the day 215 data were used to calculate the uncertainties associated with the corrosion rates over the 0−215 day period. Thus, the corrosion rates for high and medium salinity series under suboxic conditions (days 0−215) were calculated as 0.056 ± 0.002 and 0.056 ± 0.009 g cm^{-2} y^{-1}, respectively; the difference in the salinities (16.5 and 31.5) did not significantly ($p = 1.00$) affect the rate of DU corrosion. The corrosion of DU effectively ceased once SO_4^{2-}-reduction was observed, i.e., corrosion ceased under anoxic conditions, suggesting that biogeochemical conditions control the rate of DU corrosion. The suboxic corrosion rates were 7 times lower than the literature value for DU−Ti alloy in a synthetic 3.5% NaCl solution (*4*) of equivalent salinity, and from 30 to 40 times lower than the rates calculated from the in situ data (*7*). The higher corrosion rate in the 3.5% NaCl solution can be attributed to the oxic conditions. It is more difficult to explain the large difference between our microcosm corrosion rates and the previously reported in situ rates; the in situ biogeochemical conditions were not characterized due to unsuitable conditions at the time of sampling (*7*). Additionally, the in situ experiments involved a device to hold the penetrators at sediment depths of 0−15 cm (*7*), so that the coupons experienced an uncharacterised level of physical disturbance. The slower corrosion rates in the microcosm experiments reported here reflect not only the local biogeochemical conditions but also minimal physical disturbance, as would be experienced when penetrators sink through fine-grained Solway Firth sediments.

A 120 mm ("Charm 3") DU penetrator has a radius of 1.5 cm, height of 30 cm, and approximate weight of 4500 g (*6*). For simplicity, the penetrator's surface area (300 cm^2) was calculated from a perfect cylinder, not accounting for the conical tip. The corrosion rate (g cm^{-2} y^{-1}), mass and the mean surface area of a penetrator during corrosion (i.e., 150 cm^2) can be used to estimate the total corrosion time for a complete penetrator (eq 6). Under suboxic conditions, the time for a penetrator to totally corrode in both high and medium salinity systems will be 540 ± 80 years.

Uranium in the Solution Phase. The dissolved U concentrations are shown in Figure 3. There was no difference between the U concentrations in the <0.45 μm and <10 kDa fractions for the high ($p = 0.058$) and medium ($p = 0.057$) salinities, i.e., colloidal DU-oxides are not an important source of DU into this system. During the period when DU corrosion was negligible, the dissolved U concentration was less than 2 mg L^{-1}. The concentration then increased by day 103, coincident with the onset of measurable corrosion, when NO_3^--reduction was complete, and Fe(III) reduction had begun (Figure 2). At this time point, the concentration of U in the medium and high salinity microcosms was 66 and 21 mg L^{-1}, respectively. Using the inorganic carbon concentrations measured on day 1, the geochemical modeling suggests that U would be present in both the high salinity (pH: 7.1, Eh: 45 mV) and medium salinity (pH: 7.6, Eh: 30 mV) microcosms as a mixture of soluble uranyl carbonate species ($UO_2(CO_3)_3^{4-}$; $UO_2(CO_3)_2^{2-}$; $(UO_2)_2CO_3(OH)_3^-$). By day 351 the U concentration had decreased to a stable level, representing <0.1% of the total corroded U, in both the high salinity (pH: 7.8, Eh: −147 mV) and medium salinity microcosms (pH: 7.9, Eh: −172 mV). The sediment and water analyses showed that on day 500, most of the corroded DU was associated with the sediment (76 ± 5%) and <0.1% U was in the solution phase, thus the remaining corroded DU was associated with the coupon. The Hydra/Medusa modeling suggests that the low mobility UO_2 species dominates under these conditions, with a minor contribution from soluble uranyl species ($UO_2(CO_3)_3^{4-}$; $UO_2(CO_3)_2^{2-}$; $U(OH)_5^-$).

Microbial Community Profile. The high salinity sediments selected for RISA analysis suggested that DU had

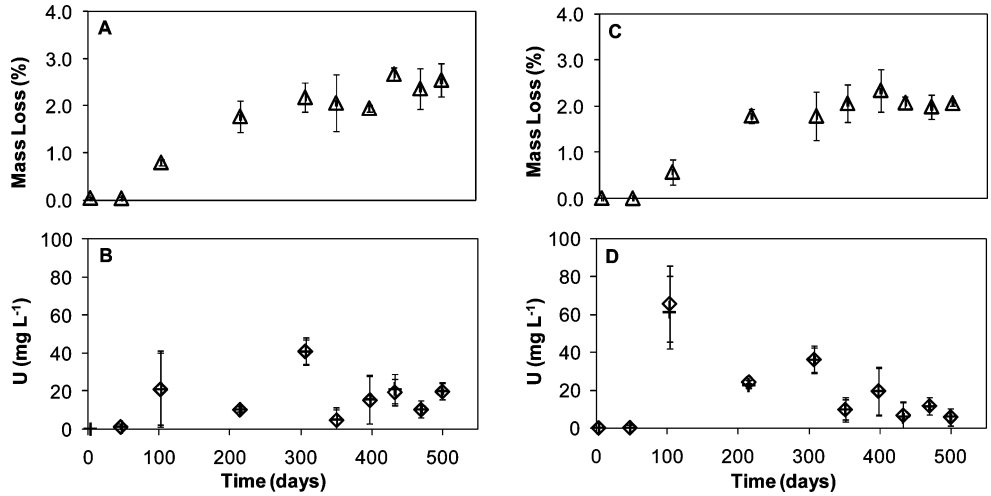

FIGURE 3. Time series data for DU corrosion in the high (A−B) and medium (C−D) salinity microcosms. (A) and (C) show mass loss (%) of DU metal from coupon (Δ). (B) and (D) show changes in <0.45 μm (+) and <10 kDa (◇) uranium in the water. Error bars show ± 1 SD ($n = 3$).

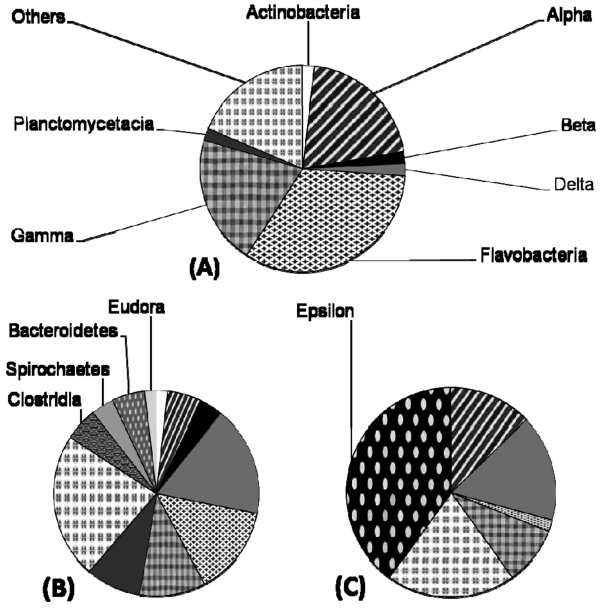

FIGURE 4. Charts show phylogenetic affiliations of clones in sediments for (A) control day 6, (B) control day 433, and (C) DU amended day 433. Phylogenetic groups are labeled once in chart order of (A) to (C). Alpha, beta, delta, epsilon, and gamma represent proteobacterial divisions.

impacted the microbial community (Supporting Information (SI) Figure 1). This warranted DNA profiling (SI Tables 1−3) which was undertaken on selected samples. Phylogenetic analysis charts (Figure 4) show bacterial groups for control day 6 (A), control day 433 (B), and DU amended day 433 (C). The controls show an increase in microbial diversity from day 6 to 433, as conditions became progressively anaerobic, with four new phylogenetic groups detected in the clone library prepared from this sample. However, the DU amended sample from day 433 shows a lower microbial diversity compared to those in either of the controls. However, a new dominant member of the microbial community appeared, affiliated with the epsilonproteobacterial group (representing 36% of the 16S rRNA genes detected in the clone library). This microbial group has previously been identified in U waste piles (*27*). Drastic loss in microbial diversity has been reported in soil when exposed to an DU oxide (U_2O_8) (*28*). In our case, there would seem to be at least one member of the microbial community that is able to adapt to the DU contamination. Microbial adaptation, even in heavily contaminated sites, has been previously observed (*29*−*31*). The dominant organism detected in the DU impacted microbial community was most closely related to *Sulfurovum lithotrophicum* (95% match over 925 bases), characterized as a sulfur-oxidizing chemolithoautotroph able to grow with elemental sulfur or thiosulfate as a sole electron donor and oxygen (5% in the gas phase) or NO_3^- as the electron acceptor. It is difficult to extrapolate the physiological profile of the organism detected from 16S rRNA gene homology, especially at only 95% homology, but selection of this dominant end member of the community could be due to resistance to potentially toxic soluble uranium corrosion products liberated in the local environment, or adaptation to the chemical environment associated with the DU, e.g., through utilization of hydrogen produced by DU corrosion, or even direct use of the depleted uranium itself as an electron donor.

Sediment Uranium Distribution and Particle Analysis. The Phosphor image for the sediment from the long-term microcosms (day 500) showed a homogeneous distribution of uranium in the sediment, with sparse localized hotspots corresponding to aggregated sediment. Representative particles were selected and analyzed by Environmental SEM-EDAX (SI Figure 2). A typical spectrum shows elements typical of marine sediments such as Fe, C, Mg, Al, Si, and Na, alongside U. The U−O−C−Si Pourbaix diagram suggests the formation of uranium silicate phases under these experimental Eh/pH conditions (*32*), which is consistent with the strong U and Si peaks observed.

Mechanism of DU corrosion in the Solway Firth. The results suggest that, as DU penetrators fired from the Kirkcudbright range sink into fine sediment areas of the Solway Firth, the biogeochemical conditions control the rate at which they corrode. The salinity (16.5 and 31.5) did not affect the corrosion rate or corrosion products formed, thus the chloride concentration, which has previously been identified as important in laboratory dissolution studies (*4, 5*), is superseded by biogeochemical conditions. Under suboxic conditions, the penetrator will corrode at approximately 0.056 g cm^{-2} y^{-1} by localized pitting and the formation of black/gray adhering UO_2. The main mechanism for U release from the penetrator is oxidation of UO_2 to U(VI) and dissolution of uranyl species such as ($UO_2(CO_3)_3^{4-}$; $UO_2(CO_3)_2^{2-}$; $(UO_2)_2CO_3(OH)_3^-$). Under more strongly reducing anoxic conditions, passivation of the penetrator occurs, preventing further corrosion. Colloidal or particulate DU-oxide corrosion products were not an important source of DU entering the

sediment or aqueous phase under the either suboxic or anoxic conditions of this geochemical system. Additionally, the corroding DU results in more reducing local biogeochemical conditions and decreases microbial population diversity.

Acknowledgments

This research was funded by the Natural Environment Research Council (grant NE/C506799/1; studentship NER/S/S2004/13082). We would like to thank Andrew Fisher, Angela Watson, Margaret Grimbly and Mustafa Sajih for technical assistance and helpful suggestions. We thank Dstl for supplying DU penetrator material and AWE for the cutting the DU.

Supporting Information Available

The ribosomal intergenic spacer analysis (RISA) profiles, tables containing the clone library DNA sequencing results, a representative backscattered electron image and ESEM/EDAX spectrum of U-rich particle. This material is available free of charge via the Internet at http://pubs.acs.org.

Literature Cited

(1) Hamilton, E. I. Depleted uranium (DU): a holistic consideration of DU and related matters. *Sci. Total Environ.* **2001**, *281*, 5–21.
(2) Dong, W.; Xie, G.; Miller, T. R.; Franklin, M. P.; Oxenberg, T. P.; Bouwer, E. J.; Ball, W. P.; Halden, R. U. Sorption and bioreduction of hexavalent uranium at a military facility by the Chesapeake Bay. *Environ. Pollut.* **2006**, *142*, 132–142.
(3) Pourbaix, M., Corrosion. In *Atlas of Electrochemical Equilibria in Aqueous Solution*; Pourbaix, M., Ed.; Pergamon Press: Oxford, 1966.
(4) Trzaskoma, P. P. Corrosion rates and electrochemical studies of depleted uranium alloy tungsten fiber metal matrix composite. *J. Electrochem. Soc.* **1982**, *129*, 1398–1402.
(5) McIntyre, J. F.; Lefeave, E. P.; Musselman, K. A. Galvanic corrosion behaviour of depleted uranium in synthetic seawater coupled to aluminium, magnesium, and mild steal. *Corros. Sci.* **1988**, *44*, 502–510.
(6) Royal Society. *The Health Hazards of Depleted Uranium Munitions. Part II. Policy Document 6/01*; The Royal Society: London, 2002.
(7) Toque, C. C. L.; Baker, A. C. *MOD DU Program - Report on the Corrosion of Depleted Uranium in the Solway Firth*, Dstl report no. dstl/ CR11679 V1.0; Dstl: Alverstoke, 2007.
(8) Konhauser, K. O.; Mortimer, R. J. G.; Morris, K.; Dunn, V., The role of microorganisms during sediment diagenesis: Implications for radionuclide mobility. In *Interactions of Microorganisms with Radionuclides*; Keith-Roach, M. J.; Livens, F. R., Eds.; Elsevier: London, 2002.
(9) Laue, C. A.; Gates-Anderson, D.; Fitch, T. E. Dissolution of metallic uranium and its alloys. *J. Radioanal. Nucl. Chem.* **2004**, *261*, 709–717.
(10) Till, B. A.; Weathers, L. J.; Alvarez, P. J. J. Fe(0)-supported autotrophic denitrification. *Environ. Sci. Technol.* **1998**, *32* (5), 634–639.
(11) Caccavo, F., Jr.; Lonergan, D. J.; Lovley, D. R.; Davis, M.; Stolz, J. F.; McInerney, M. J. Geobacter sulfurreducens sp. nov., a hydrogen- and acetate- oxidizing dissimilatory metal-reducing microorganism. *Appl. Environ. Microbiol.* **1994**, *60*, 3752–3759.
(12) Liamleam, W.; Annachhatre, A. P. Electron donors for biological sulfate reduction. *Biotechnol. Adv.* **2007**, *25*, 452–463.
(13) Oremland, R. S.; Polcin, S. Methanogenesis and sulfate reduction: competitive and noncompetitive substrate in estuarine sediments. *Appl. Environ. Microbiol.* **1982**, *44*, 1270–1276.
(14) Marsh, T. L.; McInerney, M. J. Relationship of hydrogen bioavailability to chromate reduction in aquifer sediments. *Appl. Environ. Microbiol.* **2001**, *67*, 1517–1521.
(15) Lovley, D. R.; Phillips, E. J. P.; Gorby, Y. A.; Landa, E. R. Microbial reduction of uranium. *Nature* **1991**, *350*, 413–416.
(16) Lovley, D. R.; Roden, E. E.; Phillips, E. J. P.; Woodward, J. C. Enzymatic iron and uranium reduction by sulfate-reducing bacteria. *Mar. Geol.* **1993**, *113*, 41–53.
(17) Pietzsch, K.; Babel, W. A sulfate-reducing bacterium that can detoxify U(VI) and obtain energy via nitrate reduction. *J. Basic Microbiol* **2003**, *43*, 348–361.
(18) Lovley, D. R.; Phillips, E. J. P. Reduction of uranium by Desulfovibrio desulfuricans. *Appl. Environ. Microbiol.* **1992**, *58*, 850–856.
(19) *EPA SW-846 Method 9081*; U.S Environmental Protection Agency: Washington DC: 1986.
(20) Toque, C. C. L.; Baker, A. C. *MOD DU Program - The Corrosion of Depleted Uranium in the Kirkcudbright and Eskmeals Terrestrial Environment*, Dstl report no. dstl/CR10978 V2; Dstl: Alverstoke, 2005.
(21) Lovley, D. R.; phillips, E. J. P. Availability of ferric iron for microbial reduction in bottom sediments of the freshwater tidal Potomac River. *Appl. Environ. Microbiol.* **1986**, *52*, 751–757.
(22) Stookey, L. L. Ferrozine - a new spectrophotometric reagent for iron. *Anal. Chem.* **1970**, *42*, 779–781.
(23) Graham, M. C.; Oliver, I. W.; Mackenzie, A. B.; Ellam, R. M.; Farmer, J. G. An integrated colloid fractionation approach applied to the characterisation of porewater uranium-humic interactions at a depleted uranium site. *Sci. Total Environ.* **2008**, *404*, 207–217.
(24) Cardinale, M.; Brusetti, L.; Quatrini, P.; Borin, S.; Puglia, A. M.; Rizzi, A.; Zanardini, E.; Sorlini, C.; Corselli, C.; Daffonchio, D. Comparison of different primer sets for use in automated ribosomal intergenic spacer analysis of complex bacterial communities. *Appl. Environ. Microbiol.* **2004**, *70*, 6147–6156.
(25) Islam, F. S.; Gault, A. G.; Boothman, C.; Polya, D. A.; Charnock, J. M.; Chatterjee, D.; Lloyd, J. R. Role of metal-reducing bacteria in arsenic release from Bengal delta sediments. *Nature* **2004**, *430*, 68–71.
(26) Nevell, W.; Wainwright, M. Increases in extractable sulphate following soil submergence with water, dilute sulphuric acid or acid rain. *Environ. Pollut. B.* **1986**, *12*, 301–311.
(27) Selenska-Pobell, S., Diversity and activity of bacteria in uranium waste piles. In *Interactions of Microorganisms with Radionuclides*; Keith-Roach, M. J., Livens, F., Eds.; Elsevier: London, 2002.
(28) Ringelberg, D.; Reynolds, C.; Karr, L. Microbial community composition near depleted uranium impact points. *Soil. Sediment Contam.* **2004**, *13*, 563–577.
(29) Selenska-Pobell, S.; Panak, P.; Miteva, V.; Boudakov, I.; Bernhard, G.; Nitsche, H. Selective accumulation of heavy metals by three indigenous Bacillus strains, B-cereus, B-megaterium and B-sphaericus, from drain waters of a uranium waste pile. *FEMS. Microbiol. Ecol.* **1999**, *29*, 59–67.
(30) Cerda, J.; Gonzalez, S.; Rios, J. M.; Quintana, T. Uranium concentrates bioproduction in Spain: A case study. *FEMS. Microbiol. Rev.* **1993**, *11*, 253–260.
(31) Schippers, A.; Hallmann, R.; Wentzien, S.; Sand, W. Microbial diversity in uranium mine waste heaps. *Appl. Environ. Microbiol.* **1995**, *61*, 2930–2935.
(32) Brookins, D. G., *Eh-pH Diagrams for Geochemistry*; Springer-Verlag: Berlin, 1988.

ES8021842